Increased weight gain and insulin resistance in HF-fed PLTP deficient mice is related to altered inflammatory response and plasma transport of gut-derived LPS

Effect of PLTP on gut-derived LPS

Lorène J Lebrun[1,2,3*], Gaëtan Pallot[1,2*], Maxime Nguyen[1,2,4], Annabelle Tavernier[1,2,3], Alois Dusuel[1,2], Thomas Pilot[1,2], Valérie Deckert[1,2], Isabelle Dugail[7], Naig Le Guern[1,2], Jean-Paul Pais De Barros[1,2,6], Hélène Choubley[1,2,6], Laurent Lagrost[1,2], David Masson[1,2,5], Thomas Gautier[1,2#], Jacques Grober[1,2,3#].

1. Univ. Bourgogne Franche-Comté, LNC UMR1231, F-21000 Dijon, France ; INSERM, LNC UMR1231, F-21000 Dijon, France
2. FCS Bourgogne-Franche Comté, LipSTIC LabEx, F-21000 Dijon, France
3. Agrosup Dijon, 1 esplanade Erasme, F-21000 Dijon, France
4. Department of Anesthesiology and Intensive Care, Dijon University Hospital, F-21000 Dijon, France
5. Laboratory of Clinical Chemistry, François Mitterrand University Hospital, Dijon, France
6. Lipidomic analytic plate-forme, UBFC, Bâtiment B3, Bvd Maréchal de Lattre de Tassigny, 21000, Dijon, France.
7. Faculté de Médecine Pitié-Salpêtrière, UMR1269, F-75000 Paris France

Corresponding authors: Jacques Grober & Thomas Gautier University of Burgundy, LNC UMR1231, F-21000 Dijon, France.

E-mail: Jacques.grober@agrosupdijon.fr
Thomas.gautier@u-bourgogne.fr

* *These authors contributed equally to this work and share the same first author position*

[#] *These authors contributed equally to this work and share the same last author position*

Keywords

PLTP (phospholipid transfer protein), LPS (lipopolysaccharides), lipid metabolism, obesity, inflammation, dietary fat.

Abbreviations

ApoB, apolipoprotein B; apoCII, apolipoprotein CII; apoCIII, apolipoprotein CIII; AUC, area under curve; BAT, brown adipose tissue; BW, body weight; Cer, ceramides; CM, chylomicron; EE, energy expenditure; FF, free fraction; FFA, free fatty acids; 3-HM, 3-hydroxymyristate (3-OH-C14:0); HDL, high-density lipoprotein; HF, high-fat; IL-1β, interleukin 1β; IL-6, interleukin 6; IL-10, interleukin 10; IFNγ, gamma interferon; ITT, insulin tolerance test; LBP, LPS binding protein; LF, low-fat; LDL, low-density lipoprotein; LDLR, low-density lipoprotein receptor; LPC, lysophosphatidylcholine; LPE, lysophosphatidylethanolamine; LPL, lipoprotein lipase; LPLi, lipoprotein lipase inhibitor; LPS, lipopolysaccharides; MCP-1, monocyte chemoattractant protein-1; MIP-2, macrophage inflammatory protein-2; OGTT, oral glucose tolerance test; PA, phosphatidic acid; PC, phosphatidylcholine; PE, phosphatidylethanolamine; PG, phosphatidylglycerol; PI, phosphatidylinositol; PS, phosphatidylserine; PLTP, phospholipid transfer protein; SM, sphingomyelin; SR-B1, scavenger receptor class B type I; TG, triglyceride; TLR-4, Toll-like receptor-4; TNF-α, tumor necrosis factor alpha; TRL, triglyceride-rich lipoproteins; WT, wild type.

Abstract

Bacterial lipopolysaccharides (LPS, endotoxins) are found in high amounts in the gut lumen. LPS can cross the gut barrier and pass into the blood (endotoxemia), leading to low-grade inflammation, a common scheme in metabolic diseases. Phospholipid Transfer Protein (PLTP) can transfer circulating LPS to plasma lipoproteins, thereby promoting its detoxification. However, the impact of PLTP on the metabolic fate and biological effects of gut-derived LPS is unknown. This study aimed to investigate the influence of PLTP on low-grade inflammation, obesity and insulin resistance in relationship with LPS intestinal translocation and metabolic endotoxemia. Wild-type (WT) mice were compared with *Pltp*-KO mice after a 4-month high-fat (HF) diet or oral administration of labelled LPS. On a HF diet, *Pltp*-KO mice mice showed increased weight gain, adiposity, insulin resistance, lipid abnormalities and inflammation together with higher exposure to endotoxemia compared to WT mice. After oral administration of LPS, PLTP deficiency led to increased intestinal translocation and decreased association of LPS to lipoproteins together with an altered catabolism of triglyceride-rich lipoproteins (TRL). Our results show that PLTP, by modulating intestinal translocation of LPS and plasma processing of TRL-bound LPS, has a major impact on low-grade inflammation and the onset of diet-induced metabolic disorders.

Introduction

Obesity is a pathology whose incidence is constantly increasing worldwide. It is one of the largest world's health problems (1) and is a major risk for serious non-communicable disorders including insulin resistance, type 2 diabetes, atherosclerosis and some cancers. It is now well established that high-fat (HF) diets contribute to the development of obesity (2). Moreover, excess of dietary fats not only induces weight gain but it also promotes the associated inflammatory background. Firstly, high amounts of dietary fat increase systemic exposure to potentially proinflammatory free fatty acids (FFA) and their derivatives (3). Secondly, their intestinal absorption was recently found, in both mice and humans, to facilitate the passage of bacteria-derived proinflammatory compounds such as lipopolysaccharides (LPS, endotoxins) from gut lumen to plasma (3, 4). Finally, HF diets are also known to disturb gut barrier organization and permeability and therefore to allow the entrance of luminal compounds such as the above-mentioned endotoxins. Increased endotoxemia, which results from this trans- and paracellular intestinal translocation, triggers a slight increase in plasmatic levels of pro-inflammatory cytokines such as interleukin-6 (Il-6) and tumor necrosis factor-α (TNF-α) (5) and therefore participates to the onset of a low-grade metabolic inflammation. When chronic, this low-grade inflammation alters the function of several organs such as adipose tissue, muscle, liver and intestine (6). Previous studies demonstrated that experimental induction of metabolic endotoxemia by continuous infusion of low doses of LPS is able to mimic the metabolic consequences of a HF diet. For instance, it promotes the proliferation of adipocyte precursors, the accumulation of fat mass and the subsequent development of insulin resistance (7). In addition, the deleterious effects of HF diets on intestinal permeability and on the development of metabolic endotoxemia have also been investigated. Indeed, it has been suggested that changes in gut microbiota control metabolic endotoxemia, inflammation, and associated disorders by a mechanism that could increase intestinal permeability (8, 9, and 10).

Furthermore, antibiotic treatment in mice can deeply reduce these negative effects and leads to a decreased fat mass, a lower macrophage infiltration in adipose tissue, an improved glucose tolerance but also a reduction in LPS plasma levels (11).

In the vascular compartment, plasma lipoproteins play a major protective role during inflammation and sepsis by inactivating and eliminating LPS (12). In the circulation, low-density lipoprotein (LDL) and high-density lipoprotein (HDL)-bound LPS can be taken up by the liver through the interaction of these lipoproteins (13) with their hepatic receptors, i.e., LDL-receptor (LDLR) and scavenger receptor B type I (SR-B1), respectively (14, 15) In addition to LDL and HDL, LPS can also be transported by chylomicrons (CM) (16). Indeed, CM have a high affinity for LPS and thus not only transport postprandial fat, but also significant amounts of concomitantly absorbed LPS. Interestingly, sequestration of absorbed LPS on CM reduces LPS toxicity and enhances its hepatic clearance (17).

In addition to lipoproteins, plasma proteins such as phospholipid transfer protein (PLTP), contribute to the control of endotoxemia (18, 19, and 20). PLTP was first described for its role in phospholipid transfer between lipoprotein classes (18). In previous works, we demonstrated that PLTP plays also an important role in reverse lipopolysaccharide transport pathway (RLT pathway) by promoting the association of LPS molecules to circulating HDL *in vivo* (21). Indeed, PLTP is able to transfer and exchange LPS between circulating lipoproteins (22) thereby influencing LPS detoxification by the liver. Despite its potential beneficial impact on LPS clearance, the role of PLTP in the onset of obesity and inflammation remains controversial. Indeed, in *Pltp* deficient mice, decreased binding of LPS to HDL, and thus detoxification from the body was associated with an increase in insulin secretion and a better oral glucose tolerance response (23). Moreover, some studies have demonstrated an increased PLTP activity associated with obesity and metabolic syndrome in humans whereas others have suggested that PLTP deficiency could lead to an improvement in tissue and whole-body insulin

sensitivity in mice (24, 25). In addition, a recent study has shown a beneficial effect of PLTP production by brown adipose tissue (BAT) on glucidic and lipid homeostasis (26).

Most of the protective roles of lipoproteins and PLTP on inflammation were observed in models of acute increase in endotoxemia induced by intravenous or intraperitoneal injections of LPS. However, the impact of PLTP on inflammation induced by gut-derived LPS in a context of HF diet and obesity is still unclear. The aim of the present study was to investigate this relationship in mice expressing or not PLTP and submitted to low-fat (LF) or HF diets. We show here that PLTP deficiency worsens HF-diet induced obesity and insulin resistance in mice through mechanisms involving alterations of plasma triglyceride (TG) clearance, inflammatory response and lipoprotein-mediated transport of gut-derived LPS.

Experimental procedures

Experimental animals, diets and samplings

All animal procedures were conducted in accordance with institutional guidelines and approved by the University of Burgundy's Ethics Committee on the Use of Laboratory Animals (protocol number 5459). Wild-type (WT) C57BL/6J mice and mice knocked-out for PLTP (*Pltp*-KO) on C57BL/6J background were used. Mice were matched by age (2-5 months old mice) and were housed in a controlled environment (light from 7am to 7pm, constant humidity and temperature) and were given a standard chow (LF) diet (D1250B, Research Diets Inc) or 60% high-fat diet (D12492, Research Diets Inc). Every sampling procedure (except caudal sampling) was performed under inhaled anesthesia (isoflurane) titrated to maintain spontaneous breathing. Blood was collected simultaneously in the portal vein and by intracardiac puncture in EDTA-coated tubes. Plasmas were separated by centrifugation at 8,000 x g for 10 min at 4°C and were stored at -20°C until use.

Measurements of weight gain and food intake, lean and fat masses, energy expenditure (EE) and fecal lipids content

Body mass and food intake were measured every week in mice fed with HF and LF diets. EchoMRI® was used to determine body composition through nuclear magnetic resonance (NMR) spectroscopy (fat mass and lean masses). EE measurement was performed by indirect calorimetry and adjusted according to Even and Nadkarmi (27). Total lipids in feces were extracted by Folch's method (28). Details are provided in the Supplemental Experimental Procedures.

Oral glucose tolerance test (OGTT) and insulin tolerance test (ITT)

Mice were fasted 6 hours before starting experiments. Glucose solution (150 or 200 g/L in drinking water; G8270, Sigma) or insulin solution (0.03 or 0.05 u/mL in NaCl; Humalog

100IU/mL, Lispro, Lilly) were administered at a rate of 1.5 or 2 g/kg (OGTT) and 0.3 or 0.5 u/kg (ITT), respectively. Details are provided in the Supplemental Experimental Procedures.

Conjugation of DOTA-Bodipy-NCS to LPS

DOTA-Bodipy-NCS was prepared using the method previously described (Bernhard *et al.,* 2010) (29). Briefly, LPS from *Escherichia coli* O55:B5 (Sigma-Aldrich) were incubated in the presence of one equivalent of DOTA-Bodipy-NCS solubilized in DMSO for 1 h at 37°C in a hot water bath. Labeled LPS were purified on a Superdex 75 column (GE Healthcare), concentrated with Nanosep MWCO 3 kDa (Pall).

LPS quantification

Concentrations of fluorescently labelled LPS in plasma and intestinal fractions were determined by the measurement of the fluorescence using a Perkin Elmer Wallac 1420 Victor^2 microplate reader (absorption: 485 nm / emission: 535 nm). Total LPS concentrations were also measured by liquid chromatography coupled with mass spectrometry (LCMS^2) (30, 31).

Drugs administration in mice

For LPS translocation studies, mice were gavaged with Dotaga-Bodipy-LPS concentrated at 0.5 mg/kg. For TG production kinetics, mice were treated with 0.5 g/kg Poloxamer 407 (Lutrol®, LPL inhibitor) via intraperitoneal injection to inhibit triglyceride hydrolysis. Mice were gavaged with corn oil at 10 mg/kg (Sigma-Aldrich).

Real-Time Quantitative PCR

Details are provided in the Supplemental Experimental Procedures.

Separation of plasma lipoproteins

Triglyceride-rich lipoproteins (TRL;i.e. CM and very low-density lipoprotein (VLDL), d<1.006), LDL (1.006 < d < 1.063) , HDL (1.063 < d < 1.21)) and the free fraction (FF) were separated using a 3-step sequential ultracentrifugation procedure in a TLA 100.1 rotor in a Optima™ MAX-XP Ultracentrifuge (Beckman, Palo Alto, CA). Lipoproteins were also separated by fast protein liquid chromatography (FPLC) performed on pooled plasma injected in an agarose Superose 6 column and eluted in Tris/Saline/EDTA buffer.

Plasma biochemical analyses

Cytokines, insulin, apolipoprotein CII (apoCII), and apolipoprotein CIII (apoCIII) concentrations were determined by commercially available ELISA Kits (M-CYTOMAG-70K, Millipore; 80-INSMR-CH10, Alpco; MBS923729-96, Mybiosource; MBS944394-96, Mybiosource).

Protein concentration was determined to perform normalization on samples such as gut segments. It was measured by a commercial colorimetric assay kit (Thermo Scientific™ Pierce™ BCA assay kit).

Post-heparin plasma (50 U/kg) LPL activity was measured by a commercial fluorometric kit (STA-610, Cell Biolabs, inc).

Triglyceridemia and cholesterolemia were measured by commercial photometric assay kits (Triglycerides FS, DiaSys Diagnostic Systems GmbH and Cholesterol FS, DiaSys Diagnostic Systems GmbH, respectively). Phospholipid and sphingolipid profiles were determined using the method described in Anjani *et al.* (32).

Tissue analysis

Details are provided in the Supplemental Experimental Procedures.

Statistics

Data were collected using Microsoft Excel for Office 365. Data are presented as mean ± SEM. Statistical analyses were performed using Prism 6.0 (GraphPad). To decide whether to use parametric or non-parametric statistics, the normality of distributions was assessed with the Shapiro-Wilk test (under n=7, distributions were considered to be non-normal). Statistical significance of differences between two groups was evaluated with the Mann-Whitney U test or the Student's t test (a statistical correction was applied when variances were different between groups). For more than two groups (e.g. kinetics), two-way ANOVA followed by Tukey's multiple comparisons was performed, if applicable. A value of $p<0.05$ was considered statistically significant (NS, not significant; *$p<0.05$, **$p<0.01$, ***$p<0.001$ and ****$p<0.0001$).

Results

Increased fat mass in *Pltp*-KO mice under HF diet

Weight gain, food intake, EE and fat mass were assessed in mice expressing active PLTP (WT) or not (*Pltp*-KO) which were fed for 4 months with LF or HF diet (**Figure 1** and **Supplemental, Table 1**). No significant difference in body weight was observed between WT and *Pltp*-KO mice fed with LF. Under HF conditions, both WT and *Pltp*-KO mice displayed a higher weight gain than their LF counterparts. Weight gain in *Pltp*-KO mice was significantly higher than in WT mice as early as two weeks after the onset of the diet, leading to 21.7% increase in weight gain in *Pltp*-KO mice (+60.13±3.14 vs +49.44±3.90% in WT mice; $p<0.05$) after 4 months (**Figure 1A, left)**. AUC confirmed a higher weight gain in *Pltp*-KO mice fed with HF diet (112.5±5.9 vs 119.3±7.5 arbitrary unit (au) in WT and *Pltp*-KO mice, respectively; $p<0.05$) (**Figure 1A, right**). A higher proportion of fat mass (40.7±1.7 vs 32.7±3.2% of BW in WT mice; $p<0.05$) and a lower lean mass (50.8±1.68 vs 58.9±2.86% of BW in WT mice; $p<0.05$) were observed in *Pltp*-KO mice compared with WT mice (**Figure 1B**). Additional analyses on tissue biopsies showed increased hepatic neutral lipid content and increased adipocyte size in visceral fat tissue of *Pltp*-KO mice (**Supplemental, Figure S1**). Moreover, analysis of food intake over the duration of the diet showed no significant difference between *Pltp*-KO mice and WT mice **(Figure 1C**). Similar fecal lipids content and EE were observed in both genotypes (**Supplemental, Table S1**). As a consequence, a better feed efficiency in *Pltp*-KO mice (0.05±0.02 g of body weight/kcal) compared to WT mice (0.04±0.02 g of body weight/kcal) under HF diet ($p<0.05$) was observed (**Figure 1D**).

Altered carbohydrate homeostasis in *Pltp*-KO mice under HF diet

Carbohydrate metabolism was investigated in WT and *Pltp*-KO mice (**Figure 2**). Under LF diet, oral glucose tolerance test (OGTT) led to identical response in both genotypes. HF diet led to higher glucose levels compared to LF diet in both genotypes. Glucose intolerance was more pronounced in *Pltp*-KO than in WT mice (729.8±45.13 vs 635±26.15 a.u., respectively; p=0.03) (**Figure 2A**). In similar manner, insulin tolerance test (ITT) displayed no difference under LF, an altered insulin sensitivity for both genotypes under HF and a slightly more pronounced effect in *Pltp*-KO mice (248.2±21.46 vs 197.8±14.65 a.u. in WT mice; p=0.06) (**Figure 2B**).

Plasma insulin levels under basal conditions and after glucose gavage were measured. When comparing LF fed mice, no differences were observed under basal and glucose-stimulated conditions. Under HF diet, *Pltp*-KO mice displayed a slightly higher insulinemia under basal condition which turned significant after glucose gavage (9.84±1.98 vs 4.03±1.07 ng/mL in WT mice; p=0.03) (**Figure 2C**). Thus, PLTP deficiency exacerbates HF diet-mediated glucose intolerance.

Altered plasma lipid levels in *Pltp*-KO mice under HF diet

Triglyceride (TG) levels were significantly higher in *Pltp*-KO compared to WT mice (0.88±0.04 vs 0.71±0.05 g/L, respectively; p<0.05) (**Figure 3A**) whereas plasma cholesterol was lower (1.16±0.11 vs 1.55±0.11 g/L, respectively; p<0.05) (**Figure 3B**). Decrease in plasma cholesterol was a consequence of lower amount in LDL and HDL fractions (**Figure 3C**). Plasma phospholipid profiling revealed a significant reduction in total Phospholipid (PL) in *Pltp*-KO mice (1.98 ± 0.14 vs 2.52±0.13 g/L in WT mice; p<0.05) (**Figure 3D**) especially with a marked decrease in phosphatidylglycerol (PG) (-59.8%; p<0.05) (**Figure 3E**). Within sphingolipids species, ceramide levels were almost doubled in *Pltp*-KO mice (5.73±1.20 vs

2.79±0.32 nmol/mL in WT mice; p<0.05) (**Figure 3F**). These data confirm the prominent role of PLTP in plasma lipid homeostasis, which extends beyond phospholipids to ceramides.

Oral lipid loading test led to a higher and extended TG peak in *Pltp*-KO mice compared with WT mice, with a higher TG AUC (6.23± 0.48 vs 4.55±0.38 a.u., respectively; p<0.05) (**Figure 4A**). Importantly, when TG clearance was blocked with a LPL inhibitor (LPLi), no differences in triglyceridemia was observed between the two genotypes (**Figure 4B**), indicating a key role of PLTP in TG removal from plasma.

Increased inflammation and circulating LPS and altered plasma transport of LPS in *Pltp*-KO mice

Inflammatory profiles were investigated in WT and *Pltp*-KO mice under HF diet. Plasma IL-10 and TNF-α were significantly increased in *Pltp*-KO mice when compared with WT mice (54.9±2.8 vs 37.9±3.3 pg/mL for IL-10, 23.7±2.34 vs 18.1±1.05 pg/mL for TNF-α; p<0.001 and p<0.05, respectively) (**Figure 5A**). Measurements of plasma levels of 3-hydroxymyristate (3-HM), i.e. a specific marker of LPS, showed an increased LPS concentration in *Pltp*-KO mice (**Figure 5B**). This was confirmed by calculation of AUC (6429±429 vs 7996±503 a.u. in WT and *Pltp*-KO mice, respectively; p=0.023) (**Figure 5C**).

Inflammatory profiles were also investigated in WT and *Pltp*-KO mice after an oral gavage of LPS under LF diet. IL-6 was significantly increased in *Pltp*-KO mice (392.05±80.30 pg/mL) compared to WT mice (10.01±3.23 pg/mL; p<0.05) (**Figure 6A**). Higher plasma LPS levels were observed in *Pltp*-KO versus WT mice (1.06±0.05 vs 0.80±0.04 µg/mL, respectively; p=0.0017) (**Figure 6B**). One hour after LPS gavage, free LPS (i.e. found in the lipoprotein-free fraction, FF) was significantly higher in *Pltp*-KO mice compared to WT mice (0.85±0.02 vs 0.25 ± 0.02 µg/mL, respectively; p<0.05) (**Figure 6C**). In addition, LPS concentration in the duodenum mucosa was 47.7% higher in *Pltp*-KO mice than in WT mice (13.37±0.63 vs 9.05±0.48 µg/mL, respectively; p<0.001) (**Figure 6D).** Microscopic

observations confirmed the results obtained after fluorometric assays, with a higher fluorescent signal in the proximal sections of small intestine in *Pltp*-KO mice (**Figure 6E**). Next, LPS plasma distribution was determined in portal and systemic blood at an early time-point after LPS gavage (15 minutes). In WT mice (**Figure 6F, left**), the level of TRL-bound LPS was significantly decreased in systemic blood compared to portal blood (0.24±0.08 vs 0.51±0.09 µg/mL in systemic and portal blood respectively; $p<0.0001$). The same phenomenon could be observed when considering HDL-bound LPS (0.30±0.11 vs 0.56±0.11 µg/mL, in systemic and portal blood respectively; $p=0.0005$). In *Pltp*-KO mice (**Figure 6F, right**), a similar decrease in HDL-bound LPS was observed from portal to systemic blood (0.67±0.23 vs 0.34±0.19 µg/mL in portal and systemic blood respectively; $p=0.0008$). However, regarding TRL-bound LPS, no decrease was observed in *Pltp*-KO mice while a significant drop occurred when considering free LPS (1.07±0.42 vs 0.71±0.35 µg/mL in portal and systemic blood respectively; $p=0.0082$). Overall, these results indicate that PLTP deficiency exacerbates the inflammatory status through an altered plasma transport of LPS.

Decreased LPL activity in *Pltp*-KO mice

Plasma LPL activity was quantified after oral lipid or LPS loading (**Figure 7**). A 13% decrease in *Pltp*-KO mice compared to WT mice was observed after lipid gavage ($p=0.044$) (**Figures 7A)** and a 18% decrease in *Pltp*-KO mice compared to WT mice was observed after LPS oral load ($p=0.020$) (**Figure 7B**). Gene expression of *Lpl* and plasma level of apoCII and apoCIII (LPL modulators) were determined in different conditions (**Figure 7C**). A decreased expression of *Lpl* mRNA was observed in liver (0.60±0.11 vs 1.14±0.23; $p<0.05$), ileum (0.50±0.10 vs 1.20±0.27; $p<0.05$) and muscle (0.53±0.15 vs 1.26±0.47; $p=0.07$) from *Pltp*-KO vs WT mice (**Figure 7C**). The apoCII/apoCIII ratio was significantly decreased after oral lipid loading in *Pltp*-KO mice (0.61±0.08 vs 1.04±0.12 in WT mice; $p=0.0122$) and similar trend

was observed after oral LPS challenge (0.60±0.12 vs 0.97±0.14 in WT mice; p=0.0619) (**Figure 7D and 7E**).

Finally, while gut-derived LPS accumulated to a larger extent in *Pltp*-KO mice after oral gavage (+22.5% and +32.9% at 30 and 60 mn, respectively; **Figure 8A**), administration of LPLi abrogated the increased endotoxin levels in *Pltp*-KO mice (**Figure 8B**) indicating that the altered-LPS clearance associated with PLTP-deficiency is mediated by a decrease in LPL activity.

Discussion

In line with a recent study carried out by Hoekstra *et al.* (33), we report deleterious consequences of PLTP deficiency, linked to exacerbated response to HF diet, leading to higher adiposity as well as worsened glucose and insulin tolerance. This was associated with marked alterations of plasma lipid levels and decreased postprandial triglycerides clearance. Finally, *Pltp*-KO mice display a more pronounced inflammatory status under HF conditions together with increased exposure to gut-derived LPS.

Increased weight gain in HF-fed *Pltp*-KO mice is not due to higher food intake. Feed efficiency calculation indeed demonstrates that *Pltp*-KO mice are more efficient to transform ingested kilocalories into grams of body weight. Since fecal lipid contents appear to be identical between the two genotypes, this better efficiency is not due to a better energy absorption capacity. Although a lower EE in the absence of PLTP could have been expected, no differences were observed for this parameter. However, measurements of EE were performed in specific cages in which mice were individualized. In addition, data acquisition was done over a 24-hour period which does not fully reflect the long-term effect of a four-month diet. Moreover, possible differences in gut microbiota-produced energy (34, 35), which could be modified in the absence of PLTP, have been overlooked in our EE measurements. Lastly, compared to WT, *Pltp*-KO mice display a higher adipose (low metabolic activity) to lean (high metabolic activity) mass ratio. Although this suggests that EE measurements need to be adjusted to this morphological disparity, there are still controversies about the most relevant calculation method (36). *Pltp*-KO mice have a higher amount of total fat tissues, adipocytes hypertrophy in visceral fat and higher hepatic lipid accumulation under HF conditions. Expansion of adipose tissue and liver steatosis are related to lipotoxicity which in turn is detrimental for insulin sensitivity (37, 38, 36) resulting in worsened glucose metabolism. Thus given that *Pltp*-KO mice become fatter on HFD, it is not surprising that they exhibit more pronounced alterations in glucose control.

The lipid profile of HF-fed *Pltp*-KO compared to WT mice is in line with their insulin-resistant status. Previous studies in *Pltp*-KO mice described a reduced production of TRL (40). Since it is known that HF diet increases TG levels in response to a decreased insulin sensitivity in mice (4,41), our observations suggests that increased plasma TG levels in our *Pltp*-KO model might be well the consequence of altered insulin sensitivity after a HF diet. In addition, the absence of PLTP is also associated to an increase in ceramide levels, which are known to be closely related to the pathogenesis of insulin resistance (42). Moreover, *Pltp*-KO mice display decreased HDL cholesterol levels which is also a factor associated with a loss of insulin sensitivity (43). Interpretation of changes in phospholipid profiles in PLTP deficient mice is more difficult. Although all phospholipid classes tend to decrease, we noticed a marked effect of PLTP deficiency on phosphatidylglycerols (PG) which are among the lowest abundant phospholipids in the plasma. Positive association of PG levels with fat mass was reported in obese patients (44), which is not seen here in fatter *Pltp*-KO mice. Decreased PG levels in *Pltp*-KO mice is also surprising with regard to their fatty liver phenotype, as PG elevation was observed in obese patients with non-alcoholic steatohepatitis (NASH) (32). Thus, we suggest that PLTP might have a specific preference for plasma PG remodeling independent on obesity-related metabolic status. Interestingly recent findings suggest that PG could have an anti-inflammatory effect by inhibiting toll-like receptor-4 involved in the development of low-grade metabolic diseases (45). The reduced PG levels in *Pltp*-KO mice might thus contribute to their increased inflammatory status. Ceramides are also known to be closely linked to inflammation. Therefore, the high ceramides plasma levels observed in *Pltp*-KO mice is likely a determinant of their higher inflammatory state (46).

Beyond global pro-inflammatory lipid profiles, we document a PLTP-dependent effect of pro-inflammatory LPS. HF-fed *Pltp*-KO mice have an overall increased exposure to LPS over the duration of the diet, although the difference in endotoxemia was not significant when

measured in post-absorptive state at a single time point at the end of the study. This observation highlights the importance of a regular monitoring of plasma LPS levels to clearly assess the extent of metabolic, low-grade endotoxemia (47). Although *Pltp*-KO mice were reported to display a lower inflammatory status on basal conditions (48), PLTP deficiency is known to be associated to an increased inflammation in response to LPS challenge (20). Beside previously performed IP or IV injection of LPS, we show here that either oral gavage or HF diet increase LPS in *Pltp*-KO mice. Increased LPS levels could result from higher translocation from the gut which is known to be modulated by HF diet (3, 4) or altered detoxification of circulating LPS (20). To get more insights, we developed a strategy based on the oral administration of fluorescent LPS allowing accurate monitoring in the different body compartments (30). Our observation of higher LPS concentrations and fluorescent signal in proximal gut segments of *Pltp*-KO mice suggests accelerated translocation of endotoxins. Whether a transcellular or a paracellular way for LPS crossing of the intestinal barrier (49) is affected remains to be determined. Analysis of plasma LPS distribution revealed a lack of association with TRL despite increased TG levels in *Pltp*-KO mice. This might suggest that the modalities of LPS translocation (either through packaging together with the CM in the transcellular pathway) is altered in *Pltp*-KO mice. Further studies need to be performed to precisely determinate mechanisms involved in LPS translocation in HF-fed mice.

In our model, circulating LPS was bound to HDL and TRL in WT mice whereas they were mainly found in free fraction (FF) in *Pltp*-KO mice. This is in agreement with the well-known ability of PLTP to transfer LPS onto lipoproteins, especially to HDL (50). However, we highlight here that this phenomenon occurs very rapidly upon LPS administration and most interestingly that this PLTP-facilitated mechanism also applies for gut-derived LPS binding to TRL and HDL. Previous studies have already demonstrated the protective role of TRL preventing from negative consequences of endotoxemia (51, 52). Since lipoprotein-bound LPS

are considered as an inactive form (53), defective association of gut-derived LPS to lipoproteins is likely a proinflammatory contributor in *Pltp*-KO mice. Beside inactivating circulating LPS, lipoproteins also play a key role in promoting hepatic-mediated clearance of LPS (14). Our observations reporting significant portal to central decreases in TRL- and HDL-bound LPS in WT mice are in line with the concept. Importantly, *Pltp*-KO mice displayed altered hepatic clearance of TRL-bound LPS. This might relate to an impaired LPS binding to TRL despite increased TG levels or to an impaired TRL clearance.

We demonstrate that LPL activity is decreased in *Pltp*-KO mice either after an oral lipid load or after an oral LPS administration. Moreover, exacerbated response to oral lipid load in *Pltp*-KO mice was blunted when a LPL inhibitor was administrated. These results suggest that TRL catabolism is indeed impaired in HFD *Pltp*-KO mice. In order to get more insight into the underlying causes of altered LPL activity in *Pltp*-KO mice, we studied the role of apoCII and apoCIII, LPL co-factors (54, 55) and we show that the apoCII/apoCIII balance is altered in *Pltp*-KO mice. Furthermore, *Lpl* gene expression itself was lower in the liver and ileum of *Pltp*-KO mice. Since HDL can be generated by LPL-mediated CM hydrolysis, it can be hypothesized that a decreased LPL activity could indirectly affect the association of bacterial toxins with HDL in *Pltp*-KO mice. Finally, the use of LPLi in our animals abrogated the difference in LPS clearance between *Pltp*-KO mice and WT mice reinforcing the hypothesis that altered LPL activity is a leading cause of decreased LPS detoxification in our model.

Overall, our study demonstrates that PLTP deficiency leads to less efficient detoxification of LPS but also to an exacerbated inflammatory response in the context of obesity and insulin resistance. These observations are in accordance with the concept of metabolic endotoxemia playing a key role in the aggravation of metabolic abnormalities (8). This work highlights the relationship between PLTP, TRL metabolism and low-grade inflammation as observed in metabolic diseases. Beyond the well-established implication of LPL activity in

obesity and type 2 diabetes (56), our results suggest that LPL also plays an important role in the detoxification of bacterial toxins and the attenuation of inflammation. The underlying causes of altered LPL modulation in *Pltp*-KO mice will need to be addressed in future studies.

Author contributions

GP, LJL, TG, JG, LL and DM conceived and guided the project.

GP, LJL, MN, AT, NLG, AD, VD, JPPDB, HC, TP, JG and TG carried out the experiments.

GP, LJL, JG and TG analyzed the data.

GP, LJL, JG and TG wrote the manuscript.

GP, LJL, JG, ID, DM, and TG reviewed and edited the manuscript.

All the authors have read and approved the manuscript.

Acknowledgments

The authors gratefully acknowledge JP Pais de Barros and H. Choubley from the Lipidomic platform, A. Bataille and A. Geissler from the histologic platform and V. Saint-Giorgio from the Centre de Zootechnie of the Université de Bourgogne for animal care.

Guarantors

TG and JG are the guarantors of this work and, as such, had full access to all the data in the study and takes responsibility for the integrity of the data and the accuracy of the data analysis.

Conflict of interest statement

The authors declare no existing conflict of interest.

Funding

This research was funded by grants from the Univ. Bourgogne Franche-Comté, the Institut National de la Santé et de la Recherche Médicale (INSERM), by a French Government grant managed by the French National Research Agency under the program “Investissements d’Avenir” (Lipstic Labex) and SFD-BD (Société Francophone du Diabète- Becton Dickinson).

References

1. Bouchard C. Current understanding of the etiology of obesity: genetic and nongenetic factors. Am Soc Clin Nutr. 1991;53(March):1561S-1565S.
2. Raymond SU, Leeder S, Greenberg HM. Obesity and cardiovascular disease in developing countries: A growing problem and an economic threat. Curr Opin Clin Nutr Metab Care. 2006;9(2):111–6.
3. Laugerette F, Vors C, Peretti N, Michalski MC. Complex links between dietary lipids, endogenous endotoxins and metabolic inflammation. Biochimie. 2011;93(1):39–45.
4. Petit V, Arnould L, Martin P, Monnot MC, Pineau T, Besnard P, et al. Chronic high-fat diet affects intestinal fat absorption and postprandial triglyceride levels in the mouse. J Lipid Res. 2007;48(2):278–87.
5. Gnauck A, Lentle RG, Kruger MC. The Characteristics and Function of Bacterial Lipopolysaccharides and Their Endotoxic Potential in Humans. Int Rev Immunol. 2016;35(3):189–218.
6. Michalski MC, Vors C, Lecomte M, Laugerette F. Dietary lipid emulsions and endotoxemia. OCL - Oilseeds fats, Crop Lipids. 2016;23(3).
7. Luche E, Cousin B, Garidou L, Serino M, Waget A, Barreau C, et al. Metabolic endotoxemia directly increases the proliferation of adipocyte precursors at the onset of metabolic diseases through a CD14-dependent mechanism. Mol Metab. 2013;2(3):281–91.
8. Cani PD, Amar J, Iglesias MA, Poggi M, Knauf C, Bastelica D, et al. Metabolic endotoxemia initiates obesity and insulin resistance. 2007;56(July):1761–72.
9. Winer DA, Luck H, Tsai S, Winer S. The intestinal immune system in obesity and insulin resistance. Cell Metab. 2016;23(3):413–26.

10. Cani PD, Bibiloni R, Knauf C, Neyrinck AM, Delzenne NM. Changes in gut microbiota control metabolic diet–induced obesity and diabetes in mice. Diabetes. 2008;57(6):1470–81.

11. Fujisaka S, Ussar S, Clish C, Devkota S, Dreyfuss JM, Sakaguchi M, et al. Antibiotic effects on gut microbiota and metabolism are host dependent. J Clin Invest [Internet]. 2016 Dec 1 [cited 2021 Oct 20];126(12):4430–43.

12. Levels JHM, Marquart JA, Abraham PR, Van Den Ende AE, Molhuizen HOF, Van Deventer SJH, et al. Lipopolysaccharide is transferred from high-density to low-density lipoproteins by lipopolysaccharide-binding protein and phospholipid transfer protein. Infect Immun. 2005;73(4):2321–

13. Levels JHM, Abraham PR, Van den Ende A, Van Deventer SJH. Distribution and kinetics of lipoprotein-bound endotoxin. Infect Immun. 2001;69(5):2821–8.

14. Topchiy E, Cirstea M, Kong HJJ, Boyd JH, Wang Y, Russell JA, et al. Correction: Lipopolysaccharide is cleared from the circulation by hepatocytes via the low density lipoprotein receptor. PLoS One. 2016;11(7):1–15.

15. Zannis VI, Chroni A, Krieger M. Role of apoA-I, ABCA1, LCAT, and SR-B1 in the biogenesis of HDL. J Mol Med. 2006;84(4):276–94.

16. Vors C, Pineau G, Drai J, Meugnier E, Pesenti S, Laville M, et al. Postprandial endotoxemia linked with chylomicrons and lipopolysaccharides handling in obese versus lean men: A lipid dose-effect trial. J Clin Endocrinol Metab. 2015;100(9):3427–35.

17. Xiao C, Hsieh J, Adeli K, Lewis GF. Gut-liver interaction in triglyceride-rich lipoprotein metabolism. Am J Physiol - Endocrinol Metab. 2011;301(3).

18. Zhang M, Zhai X, Li J, Albers JJ, Vuletic S, Ren G. Structural basis of the lipid transfer mechanism of phospholipid transfer protein (PLTP). Biochim Biophys Acta - Mol Cell Biol Lipids. 2018;1863(9):1082–94.

19. Deckert V, Lemaire S, Ripoll PJ, De Barros JPP, Labbé J, Borgne CC Le, et al. Recombinant human plasma phospholipid transfer protein (PLTP) to prevent bacterial growth and to treat sepsis. Sci Rep. 2017;7(1):1–16.

20. Gautier T, Klein A, Deckert V, Desrumaux C, Ogier N, Sberna AL, et al. Effect of plasma phospholipid transfer protein deficiency on lethal endotoxemia in mice. J Biol Chem. 2008;283(27):18702–10.

21. Gautier T, Lagrost L. Plasma PLTP (phospholipid-transfer protein): an emerging role in 'reverse lipopolysaccharide transport' and innate immunity. Biochem Soc Trans. 2011;39(4):984–8.

22. Hailman E, Albers JJ, Wolfbauer G, Tu AY, Wright SD. Neutralization and transfer of lipopolysaccharide by phospholipid transfer protein. J Biol Chem. 1996;271(21):12172–8.

23. Nguyen AT, Mandard S, Dray C, Deckert V, Valet P, Besnard P, et al. Lipopolysaccharides-mediated increase in glucose-stimulated insulin secretion: Involvement of the GLP-1 pathway. Diabetes. 2014;63(2):471–82.

24. Song G, Zong C, Shao M, Yu Y, Liu Q, Wang H, et al. Phospholipid transfer protein (PLTP) deficiency attenuates high fat diet induced obesity and insulin resistance. Biochim Biophys Acta - Mol Cell Biol Lipids. 2019;1864(10):1305–13.

25. Murdoch SJ, Kahn SE, Albers JJ, Brunzell JD, Purnell JQ. PLTP activity decreases with weight loss: Changes in PLTP are associated with changes in subcutaneous fat and FFA but not IAF or insulin sensitivity. J Lipid Res. 2003;44(9):1705–12.

26. Sponton CH, Hosono T, Taura J, Jedrychowski MP, Yoneshiro T, Wang Q, et al. The regulation of glucose and lipid homeostasis via PLTP as a mediator of BAT – liver communication. 2020;1–17.

27. Even PC, Nadkarni NA. Indirect calorimetry in laboratory mice and rats: Principles, practical considerations, interpretation and perspectives. Am J Physiol - Regul Integr Comp Physiol. 2012;303(5):459–76.

28. Folch J, Lees M, Sloane Stanley G. A simple method for the isolation and purification of total lipides from animal tissues. 1987;55(5):999–1033.

29. Bernhard C, Goze C, Rousselin Y, Denat F. First bodipy-DOTA derivatives as probes for bimodal imaging. Chem Commun. 2010;46(43):8267–9.

30. Duheron V, Moreau M, Collin B, Sali W, Bernhard C, Goze C, et al. Dual labeling of lipopolysaccharides for SPECT-CT imaging and fluorescence microscopy. ACS Chem Biol. 2014;9(3):656–62.

31. Pais de Barros J-P, Gautier T, Sali W, Adrie C, Choubley H, Charron E, et al. Quantitative lipopolysaccharide analysis using HPLC/MS/MS and its combination with the limulus amebocyte lysate assay. J Lipid Res. 2015;56(7):1363–9.

32. Anjani K, Lhomme M, Sokolovska N, Poitou C, Aron-Wisnewsky J, Bouillot JL, et al. Circulating phospholipid profiling identifies portal contribution to NASH signature in obesity. J Hepatol. 2015;62(4):905–12.

33. Hoekstra M, Van Der Sluis RJ, Hildebrand RB, Lammers B, Zhao Y, Praticò D, et al. Disruption of phospholipid transfer protein-mediated high-density lipoprotein maturation reduces scavenger receptor BI deficiency-driven atherosclerosis susceptibility despite unexpected metabolic complications. Arterioscler Thromb Vasc Biol [Internet]. 2020 [cited 2021 Nov 8];40(3):611–23.

34. Blaut M. Gut microbiota and energy balance: Role in obesity. Proc Nutr Soc [Internet]. 2015 Aug 21 [cited 2021 Oct 17];74(3):227–34.

35. Duca FA, Lam TKT. Gut microbiota, nutrient sensing and energy balance. Diabetes, Obes Metab. 2014;16:68–76.

36. Speakman JR, Yamada Y, Sagayama H, Berman ESF, Ainslie PN, Andersen LF, et al. A standard calculation methodology for human doubly labeled water studies. Cell Reports Medicine. 2021 Feb 16;2(2):100203.

37. Samuel VT, Shulman GI. Mechanisms for insulin resistance: Common threads and missing links. Cell. 2012 Mar 2;148(5):852–71.

38. Morigny P, Houssier M, Mouisel E, Langin D. Adipocyte lipolysis and insulin resistance. Biochimie [Internet]. 2016 [cited 2021 Oct 19];125:259–66.

39. Chavez JA, Summers SA. Lipid oversupply, selective insulin resistance, and lipotoxicity: Molecular mechanisms. Biochimica et Biophysica Acta - Molecular and Cell Biology of Lipids. 2010 Mar;1801(3):252–65.

40. Yazdanyar A, Jiang XC. Liver phospholipid transfer protein (PLTP) expression with a PLTP-null background promotes very low-density lipoprotein production in mice. Hepatology. 2012;56(2):576–84.

41. Axelsen M, Smith U, Eriksson JW, Taskinen MR, Jansson PA. Postprandial hypertriglyceridemia and insulin resistance in normoglycemic first-degree relatives of patients with type 2 diabetes. Ann Intern Med. 1999 Jul 6;131(1):27–3.

42. Chavez JA, Summers SA. A ceramide-centric view of insulin resistance. Cell Metab 2012;15(5):585–94.

43. Murdoch SJ, Carr MC, Hokanson JE, Brunzell JD, Albers JJ. PLTP activity in premenopausal women: Relationship with lipoprotein lipase, HDL, LDL, body fat, and insulin resistance. J Lipid Res. 2000;41(2):237–44.

44. Kayser BD, Lhomme M, Prifti E, Da Cunha C, Marquet F, Chain F, et al. Phosphatidylglycerols are induced by gut dysbiosis and inflammation, and favorably modulate adipose tissue remodeling in obesity. FASEB J. 2019;33(4):4741–54.

45. Choudhary V, Griffith S, Chen X, Bollag WB. Erratum: Pathogen-associated molecular pattern-induced TLR2 and TLR4 activation increases keratinocyte production of inflammatory mediators and is inhibited by phosphatidylglycerol (Mol Pharmacol (2020) 97 (324-335) DOI: 10.1124/mol.119.118166). Mol Pharmacol. 2020;97(5):354.

46. De Mello VDF, Lankinen M, Schwab U, Kolehmainen M, Lehto S, Seppänen-Laakso T, et al. Link between plasma ceramides, inflammation and insulin resistance: Association with serum IL-6 concentration in patients with coronary heart disease. Diabetologia [Internet]. 2009 Aug 11 [cited 2021 Oct 20];52(12):2612–5.

47. Boutagy NE, McMillan RP, Frisard MI, Hulver MW. Metabolic endotoxemia with obesity: Is it real and is it relevant? Biochimie. 2016 May 1;124:11–20.

48. Schlitt A, Liu J, Yan D, Mondragon-Escorpizo M, Norin AJ, Jiang XC. Anti-inflammatory effects of phospholipid transfer protein (PLTP) deficiency in mice. Biochim Biophys Acta - Mol Cell Biol Lipids. 2005 Apr 15;1733(2–3):187–91.

49. Akiba Y, Maruta K, Takajo T, Narimatsu K, Said H, Kato I, et al. Lipopolysaccharides transport during fat absorption in rodent small intestine. Am J Physiol - Gastrointest Liver Physiol. 2020;318(6):G1070–87.

50. Zhang M, Zhai X, Li J, Albers JJ, Vuletic S, Ren G, et al. The binding capability of plasma phospholipid transfer protein, but not HDL pool size, is critical to repress LPS induced inflammation. Sci Rep. 2016;6(June 2015):1–12.

51. Read TE, Harris HW, Grunfeld C, Feingold KR, Kane JP, Rapp JH. The protective effect of serum lipoproteins against bacterial lipopolysaccharide. Eur Heart J [Internet]. 1993 Dec 1 [cited 2021 Oct 17];14(SUPPL. K):125–9.

52. CJ, Kitchens RL, Wolfbauer G, Albers JJ, Munford RS. Lipopolysaccharide-binding protein and phospholipid transfer protein release lipopolysaccharides from gram-negative bacterial membranes. Infection and Immunity [Internet]. 2000 May [cited 2021 Oct 24];68(5):2410–7.

53. Harris HW, Grunfeld C, Feingold KR, Read TE, Kane JP, Jones AL, et al. Chylomicrons alter the fate of endotoxin, decreasing tumor necrosis factor release and preventing death. J Clin Invest. 1993 Mar 1;91(3):1028–34.

54. Wang CS, McConathy W, Kloer HU, Alaupovic P. Modulation of lipoprotein lipase activity by apolipoproteins. Effect of apolipoprotein C-III. J Clin Invest. 1985;75(2):384–90.

55. Wolska A, Lo L, Sviridov DO, Pourmousa M, Pryor M, Ghosh SS, et al. A dual apolipoprotein C-II mimetic-apolipoprotein C-III antagonist peptide lowers plasma triglycerides. Sci Transl Med. 2020;12(528).

56. Mead JR, Irvine SA, Ramji DP. Lipoprotein lipase: Structure, function, regulation, and role in disease. J Mol Med [Internet]. 2002 [cited 2021 Oct 20];80(12):753–69.

Figures

Figure 1. *Pltp*-KO mice have a higher fat mass under HF diet

Evaluation of body mass and energy balance during the 4 months of LF or HF in WT and *Pltp*-KO mice. **A.** Initial body weights in WT and *Pltp*-KO mice (left) and AUC of final body weight (right) (n=12-15). **B.** Weight gain and AUC in WT and *Pltp*-KO mice under LF and HF (n=10-12). **C.** Body composition in mice fed with a HF (n= 10-12). **D.** Food intake in WT and *Pltp*-KO mice under LF and HF diets (n=10-12). **E.** Feed efficiency in WT and *Pltp*-KO mice under LF and HF diet (n= 10-12). Statistical analyses were performed using the Student's t test, *$p<0.05$. All results are expressed as mean ± SEM.

Figure 2. PLTP deficiency is associated with altered carbohydrate homeostasis

Evaluation of carbohydrate metabolism in WT and *Pltp*-KO mice after 4 months of LF or HF diet. **A.** Oral glucose tolerance test (OGTT, 1.5g/kg) and blood glucose monitoring (g/L; 120min) and areas under the curves of OGTT (a.u.: arbitrary units). **B.** Insulin tolerance test (ITT, 0.5u/kg) and blood glucose monitoring (g/L; 150min) and areas under the curves of ITT (a.u.: arbitrary units). **C.** Insulin levels (ng/mL): basal (T0) and 15 minutes after glucose gavage at 1.5g/kg. Statistical analyses were performed using the Student's t test, *$p<0.05$, **$p<0.001$ and ***$p<0.0001$ (n=12-16). All results are expressed as mean ± SEM.

Figure 3. PLTP deficiency is associated with altered lipid levels under HF diet

Quantification of total plasma triglycerides (**A**) and cholesterol (**B**) in WT and *Pltp*-KO mice fed with HF for 4 months. Characterization of cholesterol in lipoproteins in plasma (from pooled samples) in WT and *Pltp*-KO mice by Fast protein liquid chromatography (**C**) Quantification of total plasma phospholipid levels (**D**) and ratios of the concentrations observed in *Pltp*-KO mice to the average of calculated concentrations in WT mice under HF for 4 months

(**E**); phospholipids: phosphatidylcholine (PC), lysophosphatidylcholine (LPC), phosphatidylinositol (PI), phosphatidylethanolamine (PE), lysophosphatidylethanolamine (LPE), phosphatidylserine (PS), phosphatidylglycerol (PG) and phosphatidic acid (PA). Quantification of total plasma sphingolipids in WT and *Pltp*-KO mice under HF for 4 months (**F**); sphingomyelin (SM) and ceramides (Cer). Statistical analyses were performed using the matched Student's t test *p<0.05 (n=10-12). All results are expressed as mean ± SEM.

Figure 4. *Pltp*-KO mice have an altered triglyceride clearance under HF diet

Quantification of plasma triglycerides (g/L) in WT and *Pltp*-KO mice fed with HF diet for 4 months, treated or not with an LPL inhibitor (LPLi; poloxamer i.p. injection 407 at 1 mg/kg). **A.** Kinetic of triglyceridemia (g/L) and AUC of triglyceridemia without LPLi in mice fed with HF for 4 months (n=11-12). **B.** Kinetic of triglyceridemia and AUC of triglyceridemia (g/L) with LPLi in mice fed with HF or 4 months (n=11-12). Statistical analyses were performed using the paired Student's t test, *p<0.05, **p<0.01 and. All results are expressed as mean ± SEM.

Figure 5. *Pltp*-KO mice have a higher inflammatory response under HF diet

Evaluation of the inflammatory status of WT and *Pltp*-KO mice fed with HF diet for 4 months **A.** Levels of cytokines (pg/mL) in mice (n=12). **B.** Quantification of circulating LPS via the measurement of 3-HM (ng/mL) by HPLC/MS/MS in mice fed with HF diet every month (n=19-22). **C.** AUC of circulating LPS in mice fed with HF diet every month (n=19-22). Statistical analyses were performed using the matched Student's t test, NS: not significant, *p<0.05 and ***p<0.001. All results are expressed as mean ± SEM.

Figure 6. *Pltp*-KO mice have a higher inflammatory response after LPS gavage

Quantification of cytokines levels, LPS plasma concentration, LPS association with lipoproteins and concentration of LPS in plasma and proximal gut segments one hour after oral LPS administration (0.5 mg/kg) and in WT and *Pltp*-KO mice. **A.** Levels of cytokines (pg/mL) one hour after LPS gavage (n=7). **B**. Plasma LPS quantification (µg/mL) after LPS gavage in mice (n=6). **C.** Mucosa LPS quantification (µg/mL) after LPS gavage in mice (n=6). **D.** Distribution of LPS (µg/mL) in lipoproteins fractions in plasma after LPS gavage (n=6). **E.** Immunofluorescence microscopy of WT (left) and *Pltp*-KO (right) mice small intestine (duodenum) cross section (immersion objective x63). **F**. Distribution of LPS (µg/mL) in portal blood and systemic blood in WT mice (left) *Pltp*-KO mice (right) 15 mn after LPS gavage (n=9)**.** Statistical analyses were performed using the matched Student's t Test, *p<0.05, **p<0.01, ***p<0.001 or a two-way ANOVA analysis **p<0.01, ***p<0.001 and **** p<0.0001. All results are expressed as mean ± SEM.

Figure 7. PLTP deficiency is associated with a lower LPL activity in mice

Kinetics of LPL activity and determination of apoCII/apoCIII ratio after oral lipid loading (10 ml/kg) or LPS gavage (0.5 mg/kg) in mice. **A.** Kinetic and AUC of LPL activity (U/mL) after corn oil gavage in mice (n=8). **B.** Kinetic and AUC of LPL activity (U/mL) after LPS gavage (n=8). **C.** Relative expression of *Lpl* mRNA / *36b4* mRNA in (n=13). **D.** ApoCII/apoCIII ratio in mice after oral lipid loading (n=10-11). **E.** ApoCII/apoCIII in mice after LPS oral administration (n=10-11). Statistical analyses were performed using the matched Student's t test, NS: not significant, *p<0.05. All results are expressed as mean ± SEM.

Figure 8. LPLi abrogates the modulatory effect of PLTP on plasma LPS in treated mice

Kinetic of plasma LPS levels (µg/mL) in mice 30 and 60 mn after LPS oral administration. **A.** Plasma LPS levels after LPS gavage (n=8). **B.** Plasma LPS levels after LPLi (P407) i.p.

injection and LPS gavage (n=8). Statistical analyses were performed using the matched Student's t test. All results are expressed as mean ± SEM.

Figure 1

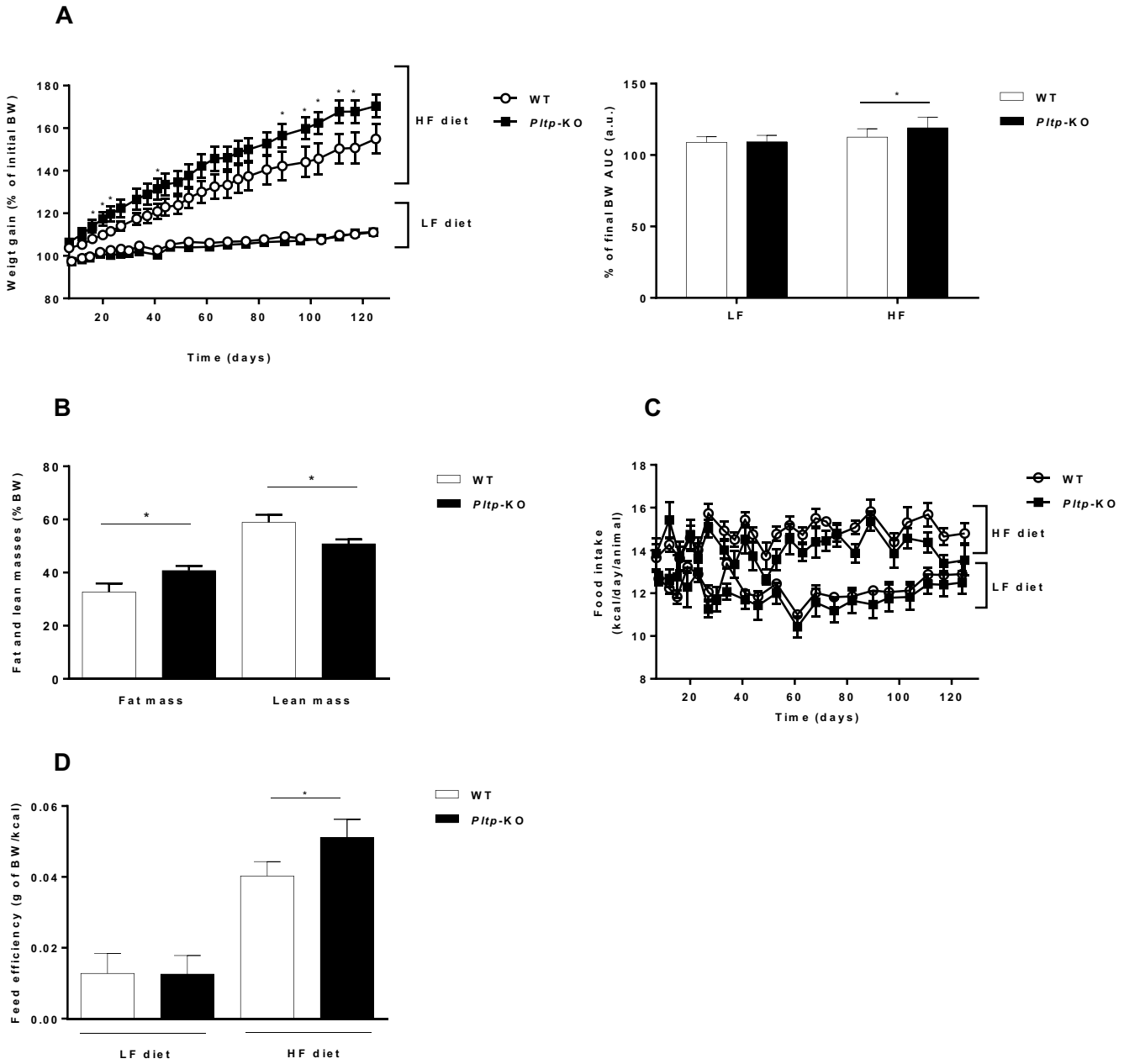
A
Weigt gain (% of initial BW)
Time (days)
HF diet
LF diet
WT
Pltp-KO
% of final BW AUC (a.u.)
LF
HF
B
Fat and lean masses (%BW)
Fat mass
Lean mass
C
Food intake (kcal/day/animal)
D
Feed efficiency (g of BW/kcal)
LF diet
HF diet

Figure 2

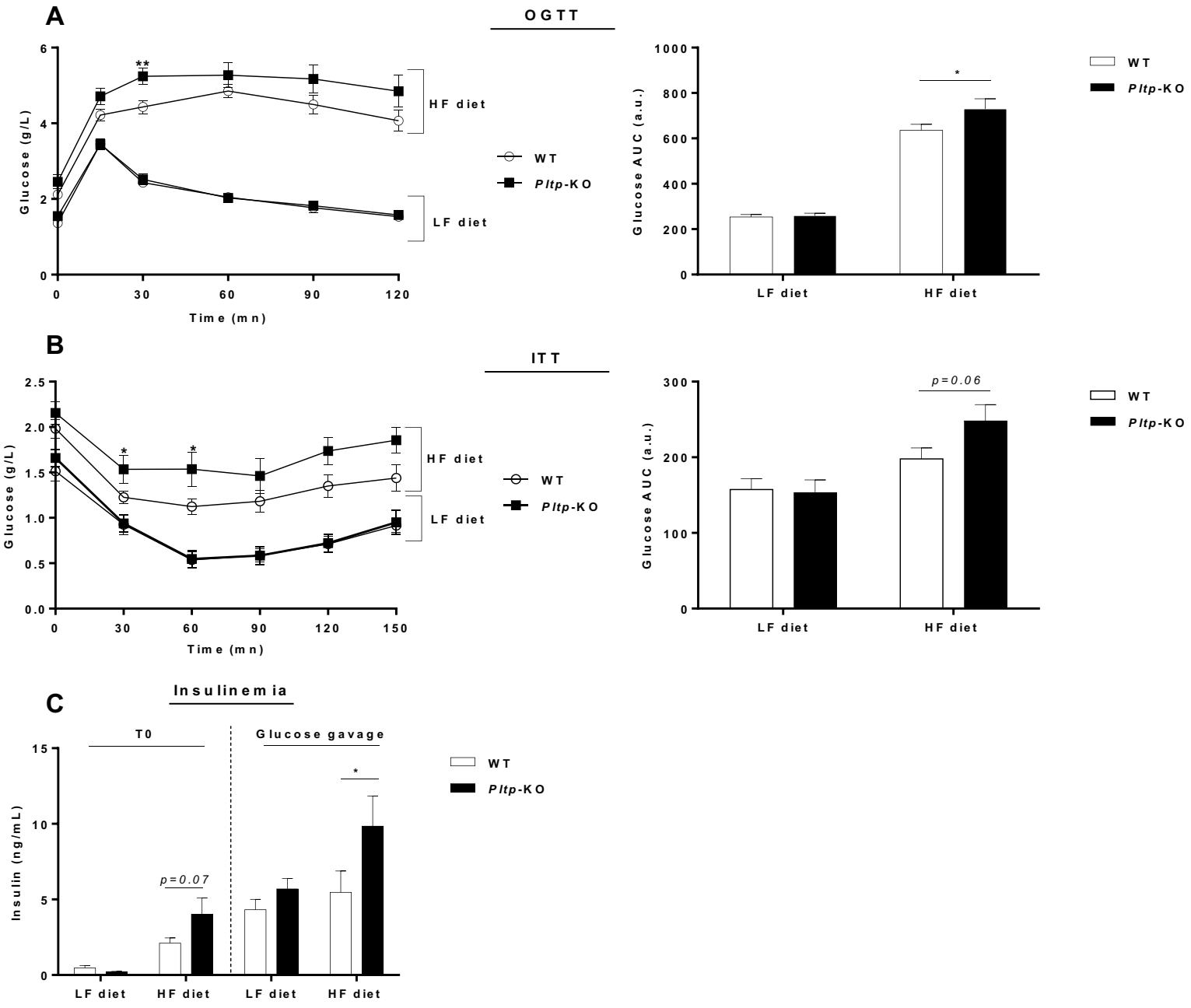
A
OGTT
Glucose (g/L)
Time (mn)
HF diet
LF diet
WT
Pltp-KO
Glucose AUC (a.u.)
B
ITT
p=0.06
C
Insulinemia
T0
Glucose gavage
Insulin (ng/mL)
p=0.07

Figure 3

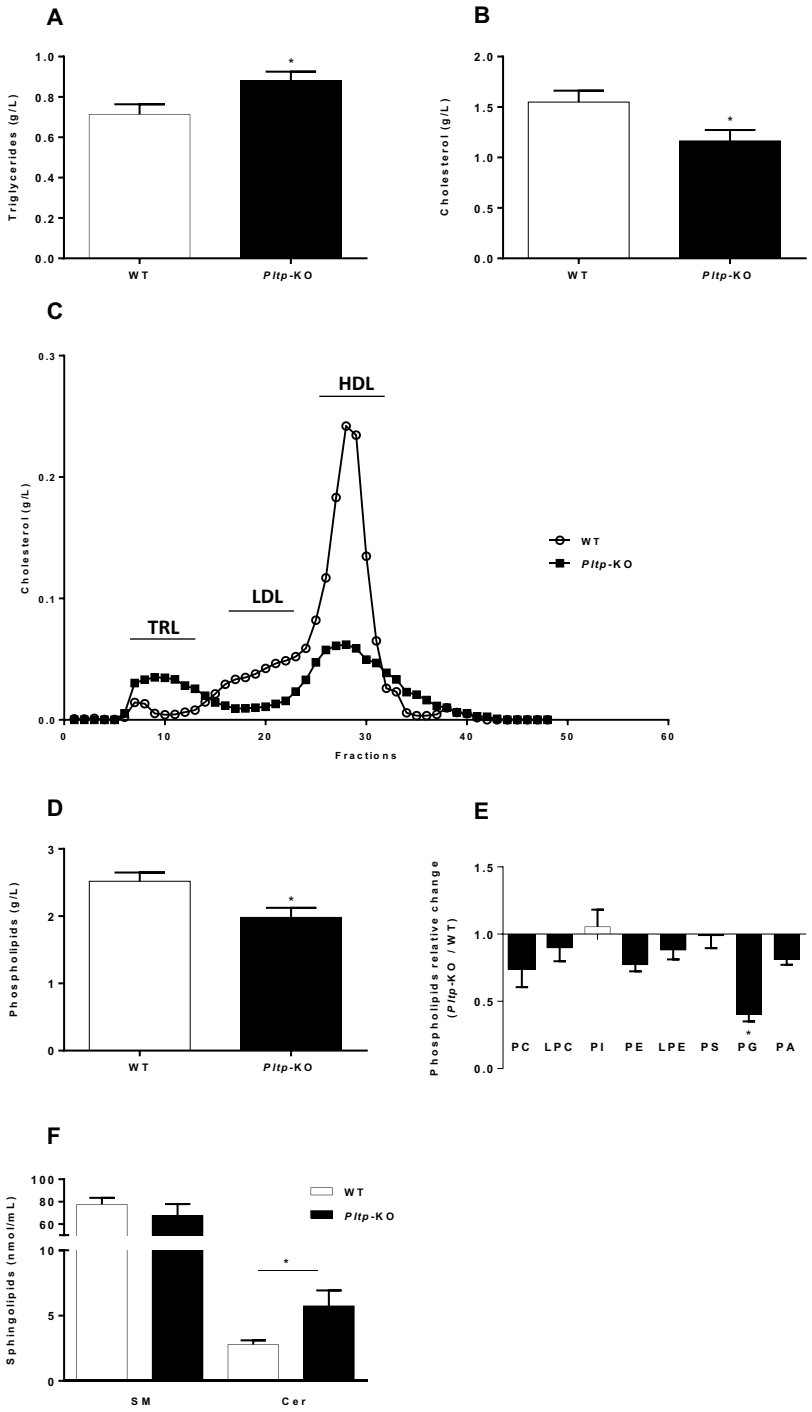
A
Triglycerides (g/L)
1.0
0.8
0.6
0.4
0.2
0.0
*
WT
Pltp-KO
B
Cholesterol (g/L)
2.0
1.5
1.0
0.5
0.0
*
WT
Pltp-KO
C
Cholesterol (g/L)
0.3
0.2
0.1
0.0
HDL
LDL
TRL
WT
Pltp-KO
0
10
20
30
40
50
60
Fractions
D
Phospholipids (g/L)
3
2
1
0
*
WT
Pltp-KO
E
Phospholipids relative change (Pltp-KO / WT)
1.5
1.0
0.5
0.0
PC
LPC
PI
PE
LPE
PS
PG
PA
*
F
Sphingolipids (nmol/mL)
100
80
60
10
5
0
WT
Pltp-KO
*
SM
Cer

Figure 4

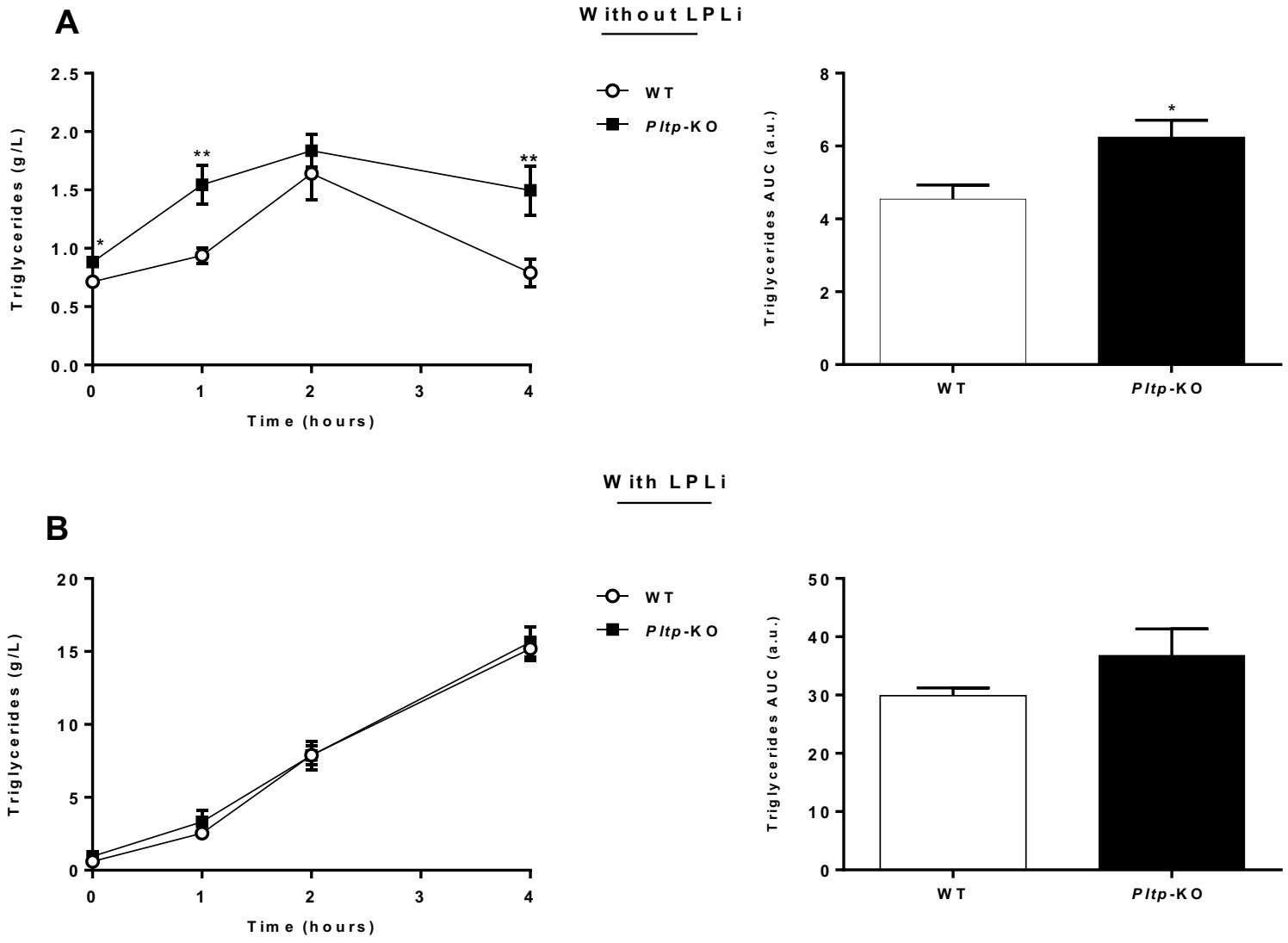
A
Without LPLi
WT
Pltp-KO
Triglycerides (g/L)
Time (hours)
Triglycerides AUC (a.u.)
B
With LPLi
WT
Pltp-KO
Triglycerides (g/L)
Time (hours)
Triglycerides AUC (a.u.)

Figure 5

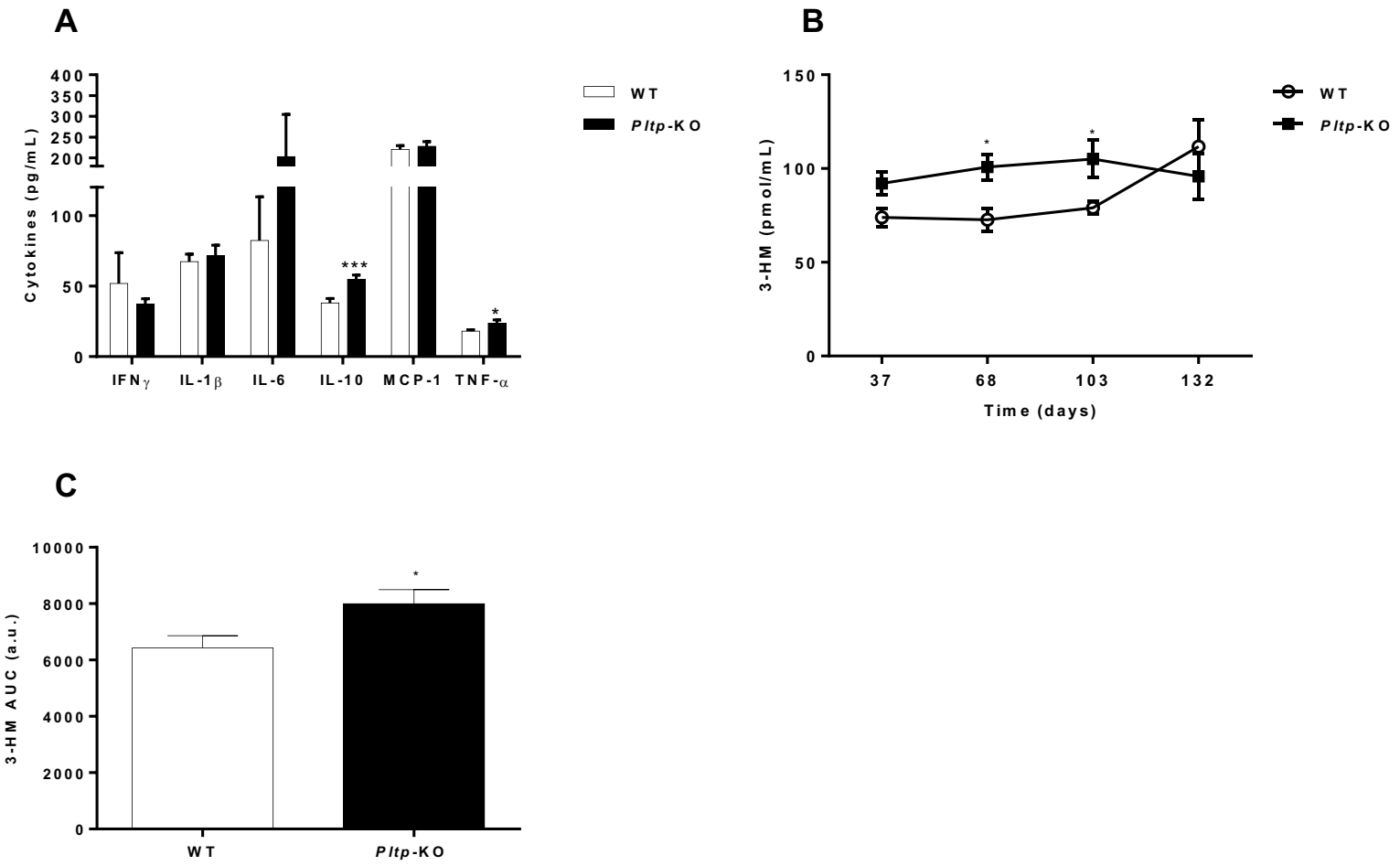
A
Cytokines (pg/mL)
400
350
300
250
200
100
50
0
***
*
IFNγ
IL-1β
IL-6
IL-10
MCP-1
TNF-α
WT
Pltp-KO
B
3-HM (pmol/mL)
150
100
50
0
*
*
37
68
103
132
Time (days)
WT
Pltp-KO
C
3-HM AUC (a.u.)
10000
8000
6000
4000
2000
0
*
WT
Pltp-KO

Figure 6

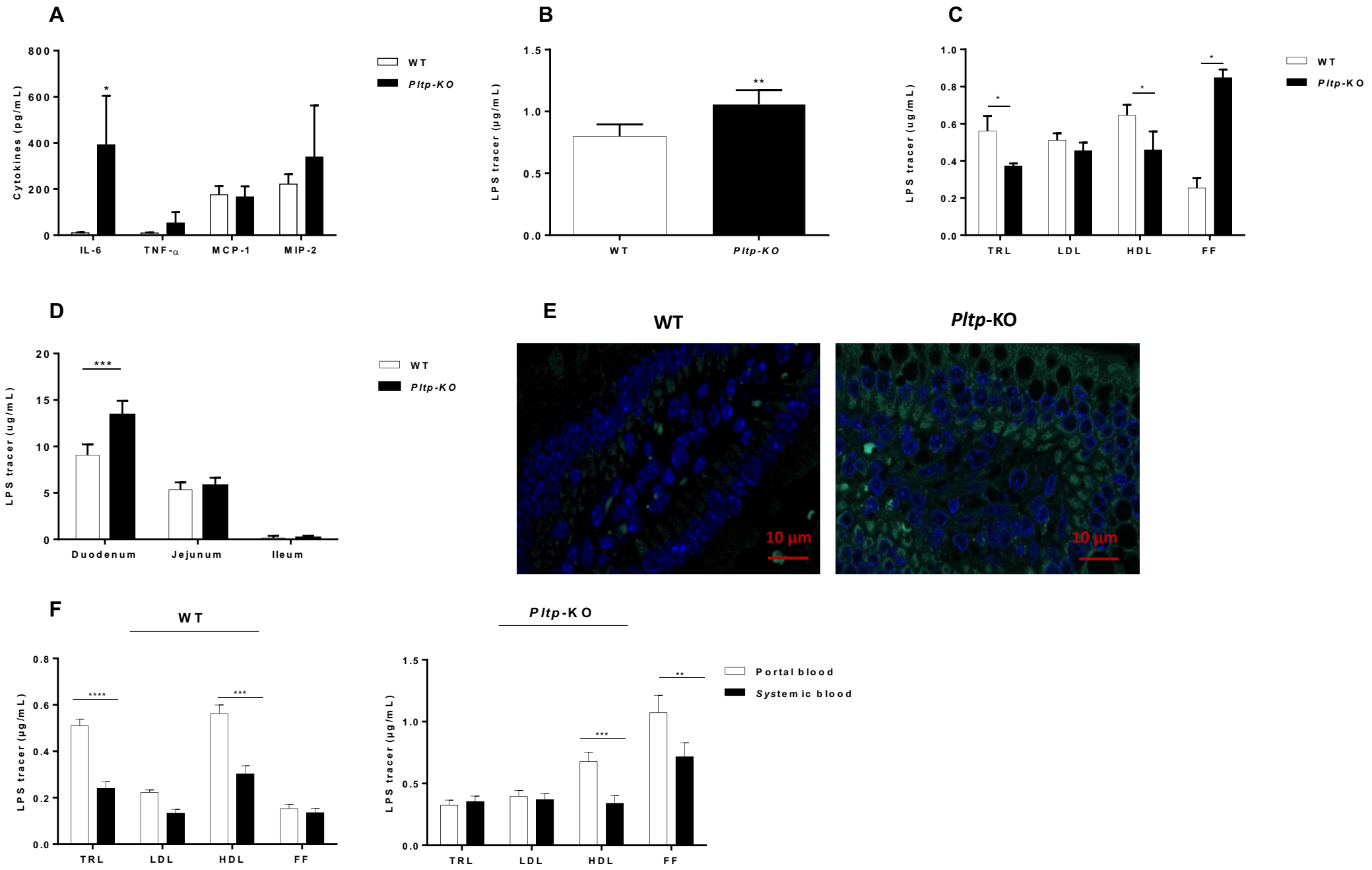
A
Cytokines (pg/mL)
800
600
400
200
0
IL-6
TNF-α
MCP-1
MIP-2
WT
Pltp-KO
B
LPS tracer (μg/mL)
1.5
1.0
0.5
0.0
WT
Pltp-KO
C
LPS tracer (ug/mL)
1.0
0.8
0.6
0.4
0.2
0.0
TRL
LDL
HDL
FF
WT
Pltp-KO
D
LPS tracer (ug/mL)
20
15
10
5
0
Duodenum
Jejunum
Ileum
WT
Pltp-KO
E
WT
Pltp-KO
10 μm
10 μm
F
WT
Pltp-KO
LPS tracer (μg/mL)
0.8
0.6
0.4
0.2
0.0
1.5
1.0
0.5
0.0
TRL
LDL
HDL
FF
Portal blood
Systemic blood

Figure 7

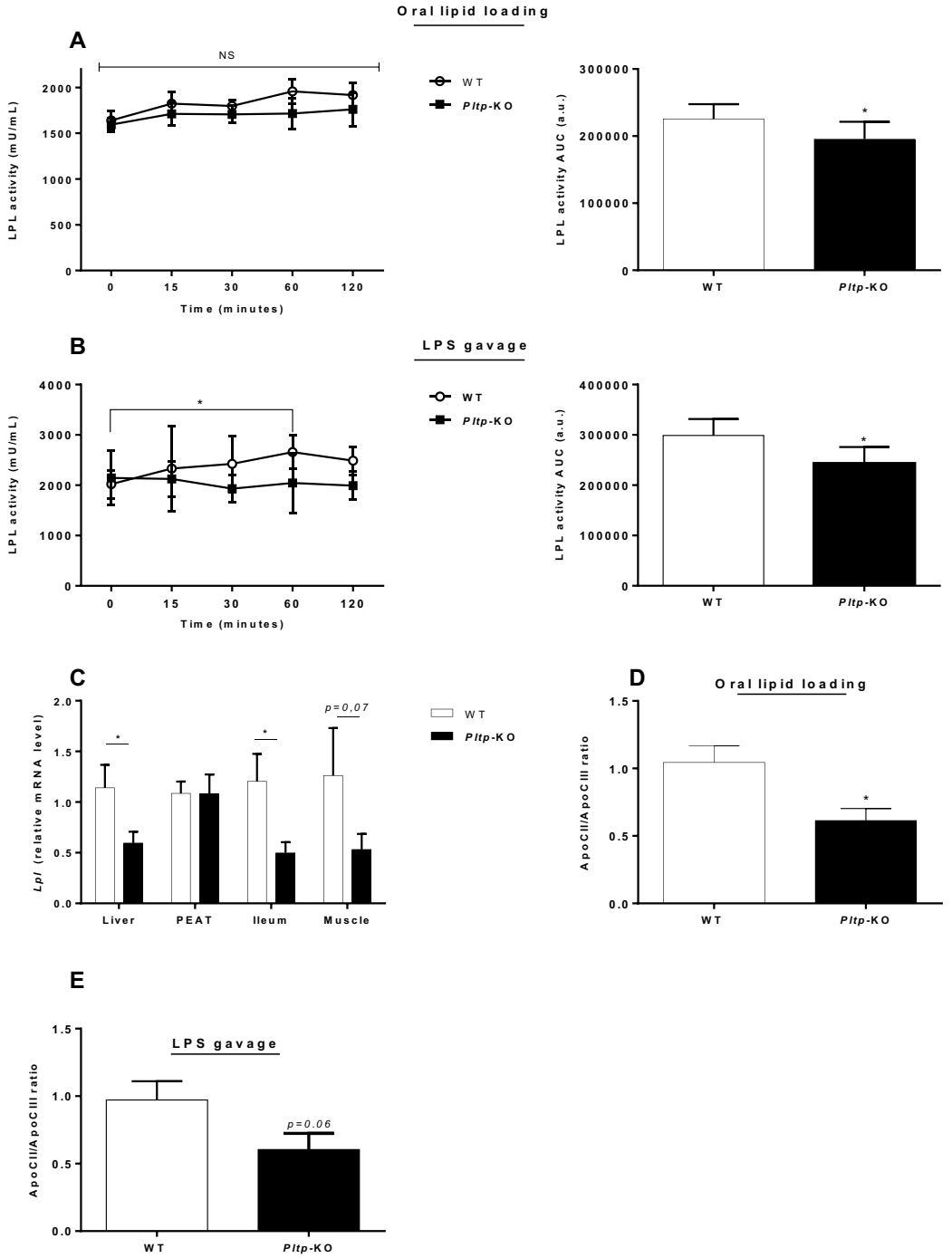
Oral lipid loading
A
NS
WT
Pltp-KO
LPL activity (mU/mL)
2000
1500
1000
500
0
0
15
30
60
120
Time (minutes)
LPL activity AUC (a.u.)
300000
200000
100000
0
*
WT
Pltp-KO
B
LPS gavage
*
4000
3000
2000
1000
C
Lpl (relative mRNA level)
2.0
1.5
1.0
0.5
0.0
p=0,07
Liver
PEAT
Ileum
Muscle
D
Oral lipid loading
ApoCII/ApoCIII ratio
E
LPS gavage
p=0.06

Figure 8

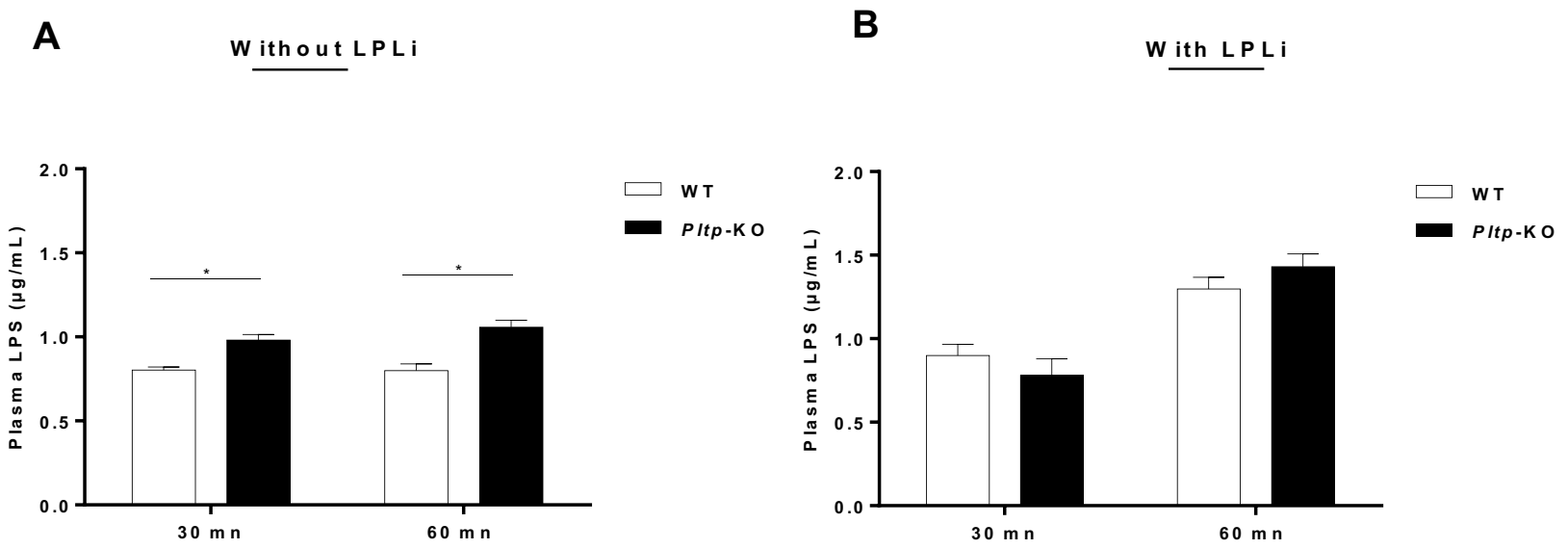
A
Without LPLi
Plasma LPS (µg/mL)
2.0
1.5
1.0
0.5
0.0
*
*
30 mn
60 mn
WT
Pltp-KO
B
With LPLi
Plasma LPS (µg/mL)
2.0
1.5
1.0
0.5
0.0
30 mn
60 mn
WT
Pltp-KO

Supplemental experimental procedures

Measurements of weight gain and food intake, lean and fat masses, energy expenditure (EE) and fecal lipids content

First, animals are weighed and then placed in a specific containment tube (EchoMRI 500T; EchoMRI, Houston, USA). Then, the tube is inserted into the device. The measurement sequence is initiated and lasts three minutes. Measurements were performed on a computer-controlled open-circuit CLAMS system (Oxymax Comprehensive Lab Animal Monitoring System; Columbus Instruments). In order to limit the effects of stress due to the modification of their environment, the mice were acclimatized to the test protocol (calorimetry cage, ventilation...) for 48 hours prior to the experiment. The measurement of the EE was carried out during 24 hours respecting the day/night cycle and with an air flow rate of 0.6 L/min. Gases evacuated from the chambers were sampled for 45 seconds every 20 minutes after a 90 seconds purging period. The volumes of oxygen (VO_2) consumed and carbon dioxide (VCO_2) produced were quantified by analyzing the sampled gases through the oxygen and carbon dioxide detector. Before starting the experiment, a calibration of the detectors was performed using a specific calibration mixture containing both oxygen, carbon dioxide and nitrogen (Air Liquide). A reference measurement with ambient air was performed every 8 measurements. The ratio of carbon dioxide production and oxygen consumption was calculated (RQ: respiratory quotient or RER: respiratory exchange ratio). At the end of the experiment the body composition data previously measured by EchoMRI® allowed the adjustment of the EE [heat production: $(3.815 + 1.232 \times RQ) \times VO_2$] to the metabolically active mass of animals (Lean mass + 0.2 Fat mass) according to the procedure described by Even and Nadkarmi. During the experiment, moves of the animals inside the cage were measured as well as the consumption of water and food in real time. Briefly, this is a simple a reliable method for extraction of fecal lipids, more particularly

phospholipids and neutral lipids such as tripalmitin, lecithin, calcium stearate, cholesterol, cholesteryl palmitate, and a mixture of all of these. Fecal samples are homogenized with a mixture of chloroform, methanol, acetic acid and water. The extract is washed with water to remove non-lipidic impurities extracted by the solvents. The washing procedure also removes the methanol and acetic acid, leaving the lipids in the chloroform layer. Recoveries of known lipids mentioned above added to fecal samples before extraction averaged 99 percent.

Oral glucose tolerance test (OGTT) and insulin tolerance test (ITT)

Glucose was administered orally through a cannula of gavage and insulin was injected via IP. Blood glucose was measured over time through the tail vein and with a blood glucose monitor (OneTouchUltra, Lifescan). Measurements was taken before gavage and 15, 30, 60, 90, 120 and 210 minutes after gavage for OGTT. Measurements was taken before injection and 30, 60, 90, 120 and 150 minutes after injection.

Real-Time Quantitative PCR

Duodenum, jejunum, ileum, colon, liver, muscle and peri-epididymal adipose tissue were immediately snap frozen (immersion in liquid nitrogen) after harvest and stored at -80°C until RNA extraction. Total RNA was isolated using TRIzol reagent. RNA extraction included a DNAse treatment step. RNA was quantified using the NanoDrop 1000 spectrophotometer (Thermo Scientific), and 500 ng of RNA from each sample was reverse transcribed using the High-Capacity cDNA Reverse Transcription Kit (Multiscribe® reverse transcriptase, 4368813, Applied Biosystems) according to the manufacturer's instructions. Quantitative PCRs were performed using StepOnePlus (Real-Time PCR System, Applied Biosystems), TaqMan® (4324018, Applied Biosystems) or SYBRGreen® (4367659, Applied Biosystems)

technologies. The mRNA level was normalized to levels of *Gapdh* or *Rplp0* mRNA and the results were expressed as relative expression levels using the 2-ΔΔCt method.

LPS quantification

This method relies on the quantification of 3HM. Samples (30 µL) were mixed with 4 µL of 3-OH-tridecanoic acid used as internal standard (1 µg/µL in ethanol) and 300 µL of hydrochloric acid 8M. After a 3 hours hydrolysis step at 90 °C, free fatty acids were extracted with 600 µL of distilled water and 5 ml of hexane/ethyl acetate (3/2 v/v). After evaporation of the organic phase, dried extract was solubilized in ethanol (50 µL) and 3 µL were injected on a SBC18 2,1x50 mm, 1,8 µm column and connected to an Infinity 1290 HPLC system (Agilent Technologies). Separation of 3OH-free fatty acids was achieved at 45 °C using ammonium formate 5 mM / formic acid 0,1% as eluent A and acetonitrile 95% as eluent B. The elution gradient was set-up at a flow rate of 0,4 ml/min as follows: 55% A for 0,5 min, up to 100 % B in 2,5 min and maintained at 100 % B for 5 min.MS/MS detection was performed in negative mode using a QqQ 6490 triple quadruple mass spectrometer equipped with a JetStream ESI source (Gas Temperature 290°C, Gas Flow 19 l/min, Nebulizer 20 psi, Sheath Gas Heater 175 °C, Sheath Gas Flow 12 l/min, Capillary Voltage 2000 V, Charging 200 V). The mass spectrometer was set up in the selected reaction monitoring mode for the quantification of selected ions as follows: for 3-hydroxytetradecanoic acid (3HM), precursor ion 243.2 Da, product ion 59 Da, for 3-hydroxytridecanoic acid (IS), precursor ion 229.2 Da, product ion 59 Da, Collision energy and Cell Acceleration was set at 12 V and 2 respectively.

Tissue analysis

Intestinal sections (duodenum, jejunum and ileum) from mice were put in paraformaldehyde solution 4% (Cell Store Pot, 10% neutral buffer formalin, 60 ml). Intestinal

sections were then cut, fixed in acetone at −20 °C for 10 min, and mounted in Vectashield fluorescent mounting medium with DAPI (Vector). Slides were observed with an Axio Imager M2 epifluorescence microscope (Zeiss) with excitation at 485 nm and emission at 535 nm for Bodipy.

Supplemental table and figure

Table

	WT	*Pltp*-KO	n (per group)	*p* values
Energy expenditure (EE)	14.93±0.60	16.62±0.87	12	0.12
Fecal lipids content	0.02±0.01	0.02±0.01	4	0.60

Table S1. Energy balance of *Pltp*-KO mice is not altered under HF diet

Assessment of energy balance in WT and *Pltp*-KO mice after 4 months of HF diet: energy expenditure (EE) (kcal/day/animal) and fecal lipids content (mg/g). Statistical analyses were performed using the Student's t test. All results are expressed as mean ± SEM.

Figure

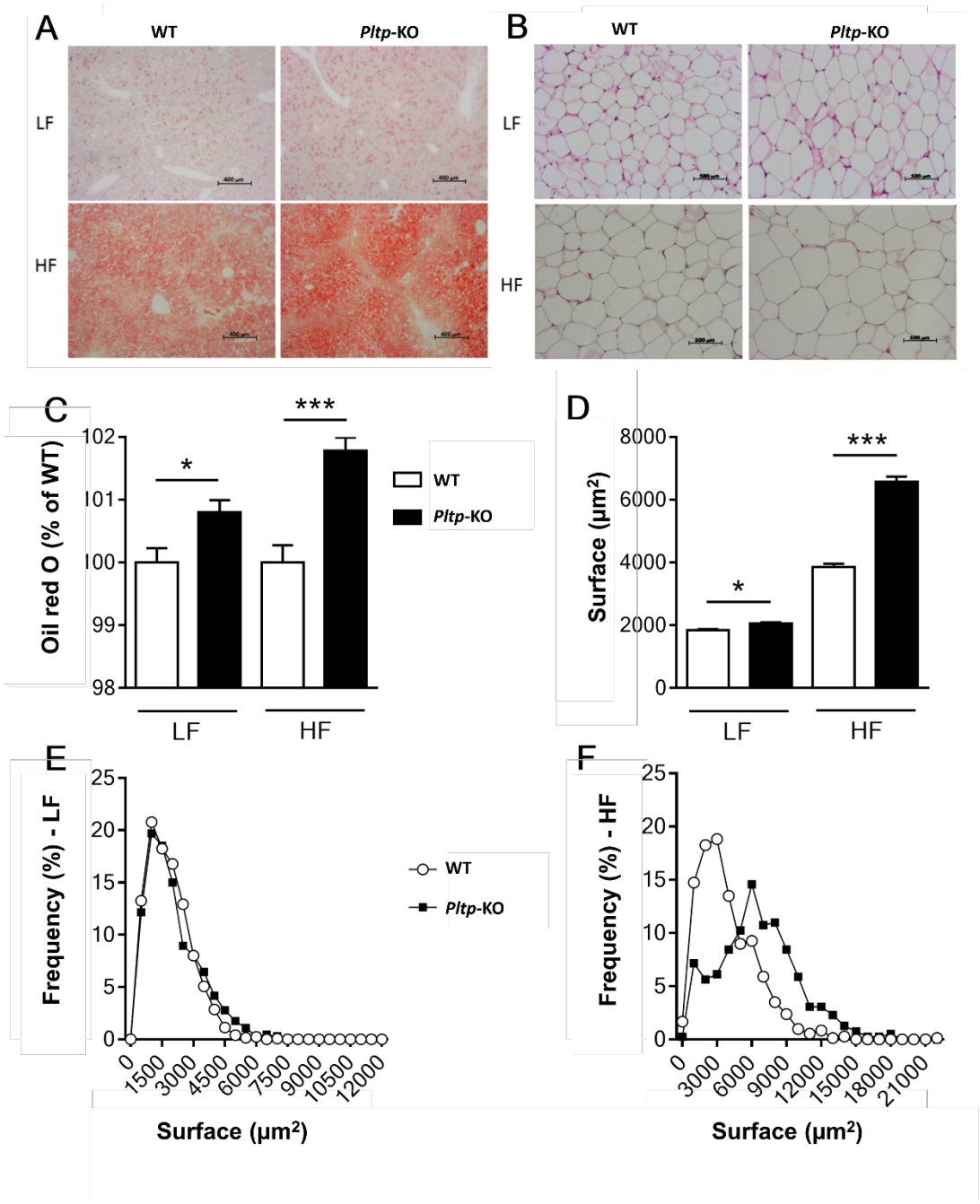

Figure S1. Tissue analyses (liver and adipose tissue) in WT and *Pltp*-KO mice under LF or HF. **A** Microscopy of mice liver. **B.** Microscopy of mice adipose tissue. **C.** Oil red O (% of WT) analyses in mice. **D.** Adipocyte surface in mice (µm^2). **E.** Distribution of adipocyte according to their surfaces in mice under LF. **F.** Distribution of adipocytes according to their surfaces in mice under HF. Statistical analyses were performed using the Student Test, *p<0.05 an *p<0.001. All results are expressed as mean ± SEM.